
# Magnetism Demonstrations:
# Magnetic Signatures of Some Common States of Materials
# (Vibrating Sample Magnetometer Option)

http://education.qdusa.com/experiments.html

**Prof. Stephen Tsui[1] and Dr. Neil Dilley[2]**
**California State University San Marcos[1]**
**Birck Nanotechnology Center, Purdue University[2]**

*The demonstration of magnetic ordering phenomena via acquisition of real data can be a powerful tool in the condensed matter classroom and laboratory. This module, written with instructors in mind, offers fundamental demos that characterize magnetic ordering behavior using readily attainable materials. This can be a point of reference for developing lectures or new laboratory activities.*

## Student Learning Outcomes:

Students will observe the magnetization vs. temperature and magnetic field behaviors for:

- paramagnetism
- ferromagnetism
- antiferromagnetism
- diamagnetism
- superconductivity

## Background and Experiment:

This demonstration module provides a point of reference for obtaining data on the several magnetic behaviors most commonly discussed in courses. In fact, the materials measured here were inspired by the Quantum Design Periodic Table of Elements, which shows the known ordering of the elements (Figure 1) [1]. It is highly recommended to read "Fundamentals of Magnetism and Magnetic Measurements" by Mike McElfresh [2] as an overview of magnetic phenomena and experiment.

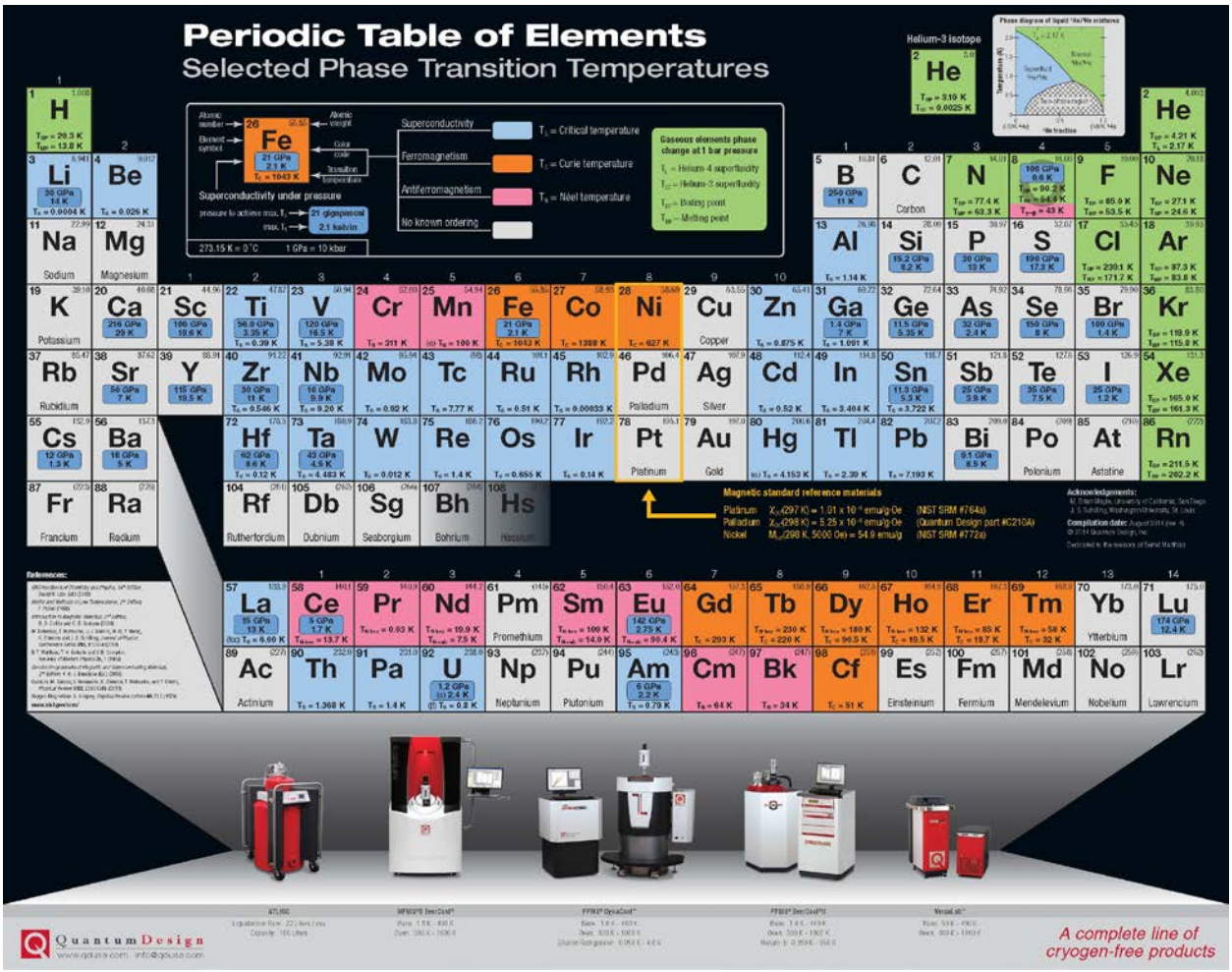


Figure1: The Quantum Design Periodic Table of Elements located at http://www.qdusa.com/sitedocs/Quantum_Design_Periodic_Table.pdf

All the measurements in this module were performed using the Vibrating Sample Magnetometer (VSM) option on the VersaLab. Please refer to the VSM manual to properly install and measure samples. Samples may be mounted on either the brass holder or quartz paddle that comes with your VSM. Ge 7031 varnish is a convenient medium to adhere samples to the holders, but time and care must be used to clean the varnish off with alcohol or toluene. You may also use powder capsules clamped into the brass holder or Kapton tape to mount samples. Whatever you choose, be aware that mounting media may contribute to the measured signal, so it is best to establish what your experimental background is. For example, even the brass holder itself can provide a contribution on the order of 10 μemu at very high applied magnetic fields (Figure 2). Please read Application Note 1096-306 [3] on VSM sample mounting on the QD website for more guidance on this topic.

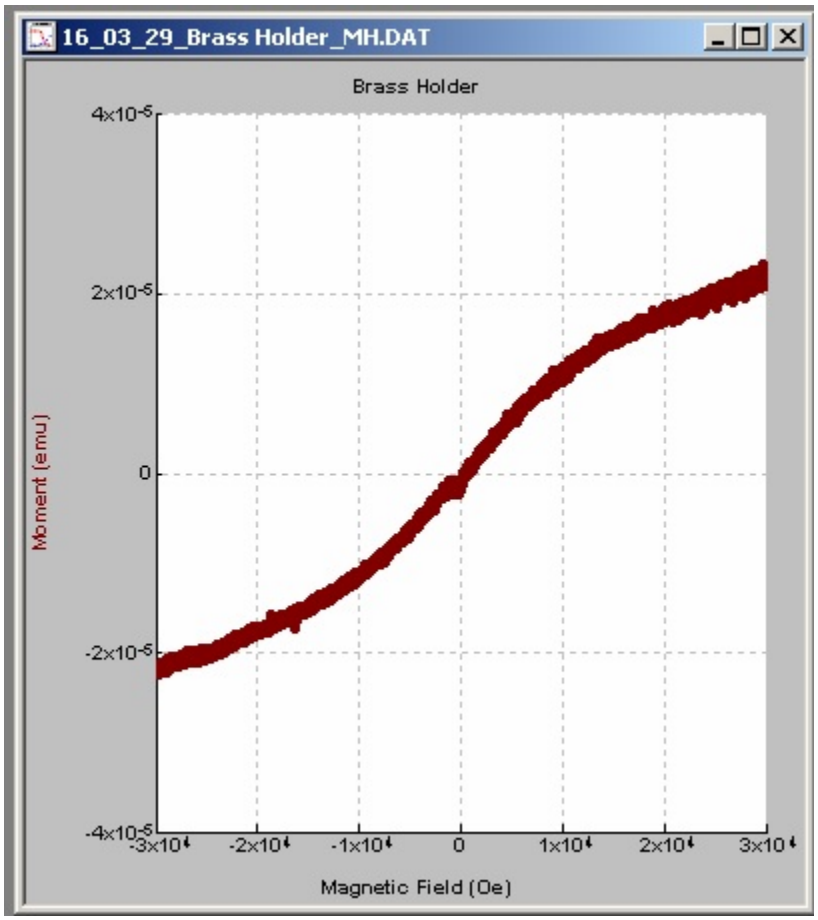


Figure 2. Moment vs. field for the brass holder without sample. Always determine the sample holder background before performing measurements.

A list of materials and supplies is included at the end of this module.

It should be noted that most literature reports magnetization *M* in emu/g, but the plots shown in this module are raw data reported in emu.

## Paramagnetism:

A paramagnetic material contains atoms with free magnetic moments, e.g., those associated with unpaired electrons, that are disordered due to thermal energy [2]. In the absence of magnetic field, the net magnetization is zero. In the presence of an applied magnetic field, the moments will align with the field and result in a net magnetization. However, this magnetic alignment will be in competition with the randomizing effects of thermal fluctuations, such that the net moment will be reduced at higher temperatures. It was Pierre Curie who first reported this behavior experimentally [4], and the magnetization vs. temperature behavior for paramagnets is described by the Curie-Weiss law,

$$\frac{1}{\chi} = \frac{T-\theta}{C} \qquad (1),$$

where $\chi$ is the magnetic susceptibility, T is temperature, C is the Curie constant, and $\theta$ is the Weiss constant. The 1/T dependence of the magnetic susceptibility captures the effects due to thermal fluctuations and is known as the Curie law. The Weiss constant is associated with the effects of the material's molecular field at low temperature, leading to a net magnetic interaction, either ferromagnetic or antiferromagnetic, within the material. When plotting $1/\chi$ vs T, a Curie type paramagnet will have a zero y-intercept, whereas a Curie-Weiss paramagnet will have a y-intercept at $\theta$.

Below is a measurement of magnetic moment vs. temperature performed on $Dy_2O_3$ (Figure 3), which is often used as a paramagnetic standard material [5]. The $Dy_2O_3$ powder was encapsulated and mounted in a brass holder. The field was set to H = 1000 Oe, and temperature was swept at a rate of 1 K/minute.

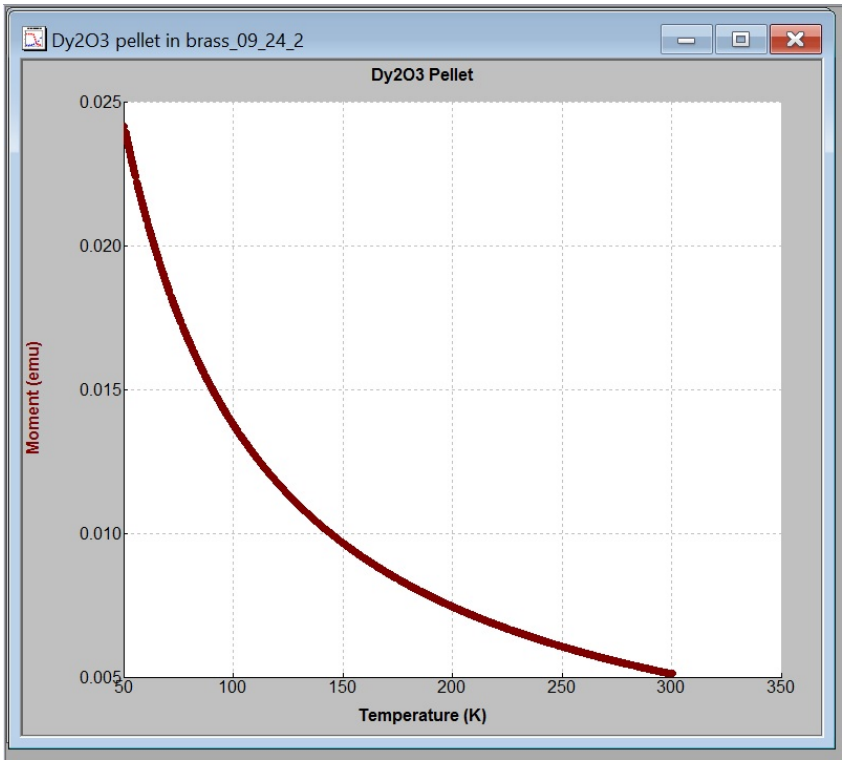


Figure 3. Measurement of magnetic moment vs. temperature using H = 1000 Oe for $Dy_2O_3$ sample.

Dividing the magnetic moment by the applied field yields the susceptibility, the inverse of which is plotted vs temperature in Figure 4 in order to determine the value of $\theta$, approximately -18 K.

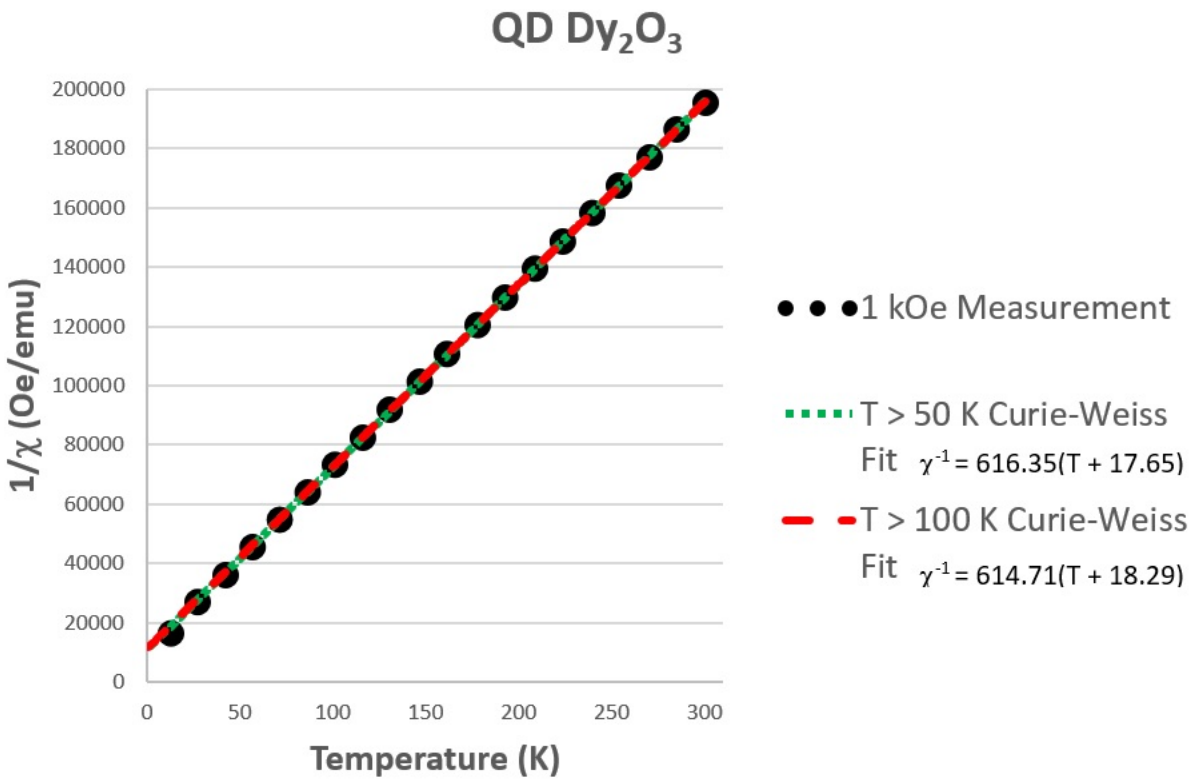


Figure 4. Fitting the data in Figure 1 to determine the Weiss constant.

The magnetic moment vs. H curve for a paramagnet is linear and reversible, since the net magnetization is field dependent as mentioned above.

As an additional example, the moment vs. field for a small sample of Ti foil is plotted in Figure 5. The sample was mounted on a quartz paddle using a very small amount of GE varnish. The data obtained displays the expected intrinsic linear behavior of the M(H) curve, but we also note that there is a slope change in the low field region, which is an extrinsic contribution to the M(H) that may be attributed to magnetic impurities in the sample.

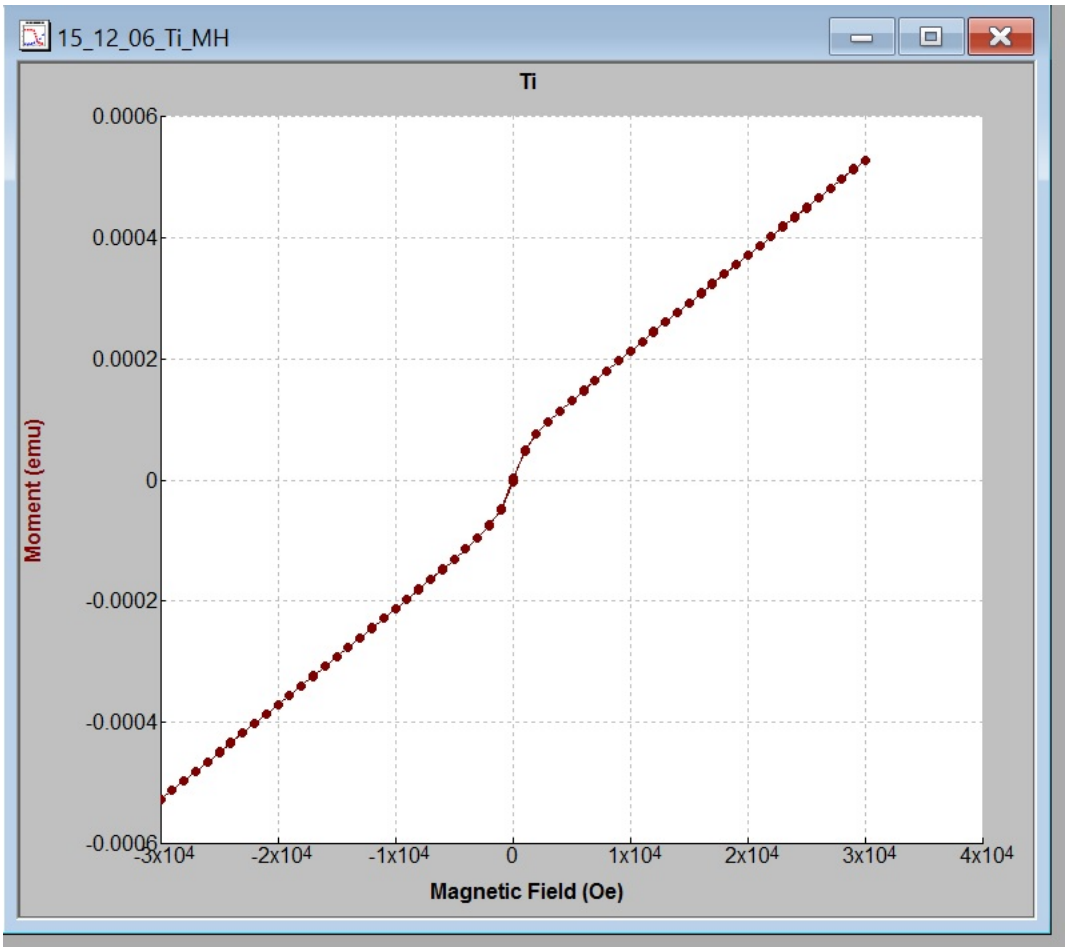


Figure 5. Moment vs. field for Ti foil at 300 K showing paramagnetic behavior, with a low field kink that may be due to sample impurities.

Note that this sample of Ti foil has a small moment, especially when compared to the $Dy_2O_3$. For such samples, the choice of mounting medium becomes extremely important.

## Ferromagnetism:

A ferromagnet may be regarded as a paramagnet with a very large molecular field [4], which leads to a net long range magnetic ordering even in the absence of an external applied magnetic field. The tell-tale sign of ferromagnetism is a hysteretic S-shaped M(H) curve. As the strength of the applied magnetic field increases, the net magnetization increases nonlinearly until a saturation field value. When the magnetic field is reduced, the material does not simply return to its previous state but rather contains a remanent magnetization that will change the curve history. In order to bring the magnetization to zero, a coercive field must be applied. Drawing from the discussion of paramagnets, it should be no surprise that sufficient thermal energy will disorder a ferromagnet and render its behavior to that of a Curie-Weiss

paramagnet. The temperature above which this occurs is the Curie temperature $T_C$.

Gd is a readily available material with a Curie temperature of 293 K, as can be seen in the Quantum Design periodic table of elements (Figure 1). An effective demonstration of the Curie temperature is to measure the magnetic moment vs. H above and below $T_C$ (Figure 6). We mount the Gd foil using Kapton tape onto a quartz paddle. The sweep rate was 10 Oe/second.

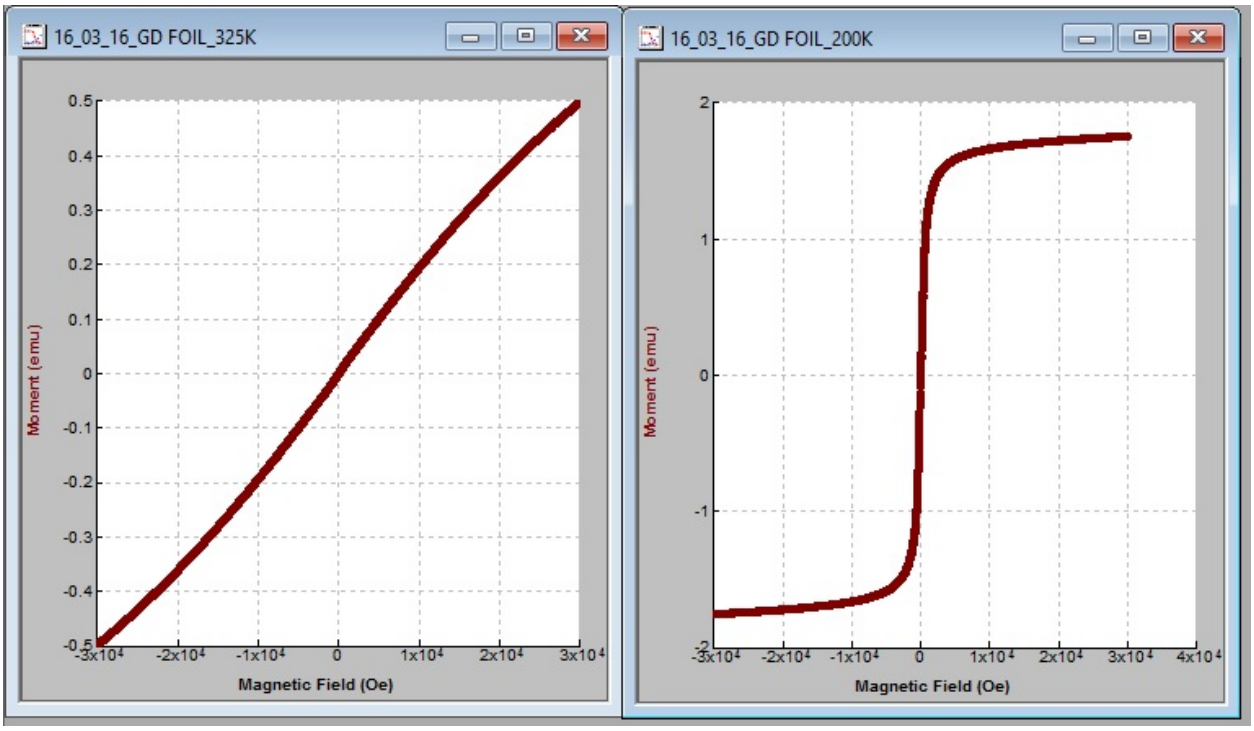


Figure 6. (left) Gd foil measured at 325 K, above the Curie temperature; (right) Gd. Foil measured at 200 K, below the Curie temperature.

The change in behavior from paramagnetic (linear) to ferromagnetic (S-shaped) behavior is quite dramatic. The literature reports that Gd has little hysteretic behavior [6].

We also perform a moment vs. temperature plot on the Gd foil (Figure 7). The measurement can be performed zero field cooled (ZFC) or field cooled cooled (FCC). In a ZFC sequence, the sample is cooled in the absence of magnetic field, and the moment is measured while warming up in the presence of the applied field. In a FCC sequence, the sample is cooled and measured while in the presence of magnetic field during the cooling. The data reveals the value of the Curie temperature via the slope change near 293 K. At high temperatures, the curves are similar. However, the ZFC curve shows a down-turn of the moment at low temperature, whereas the FCC curve shows a flat moment at

low temperature. This is associated with the magnetic anisotropy in the material, which is relatively low in this sample [7].

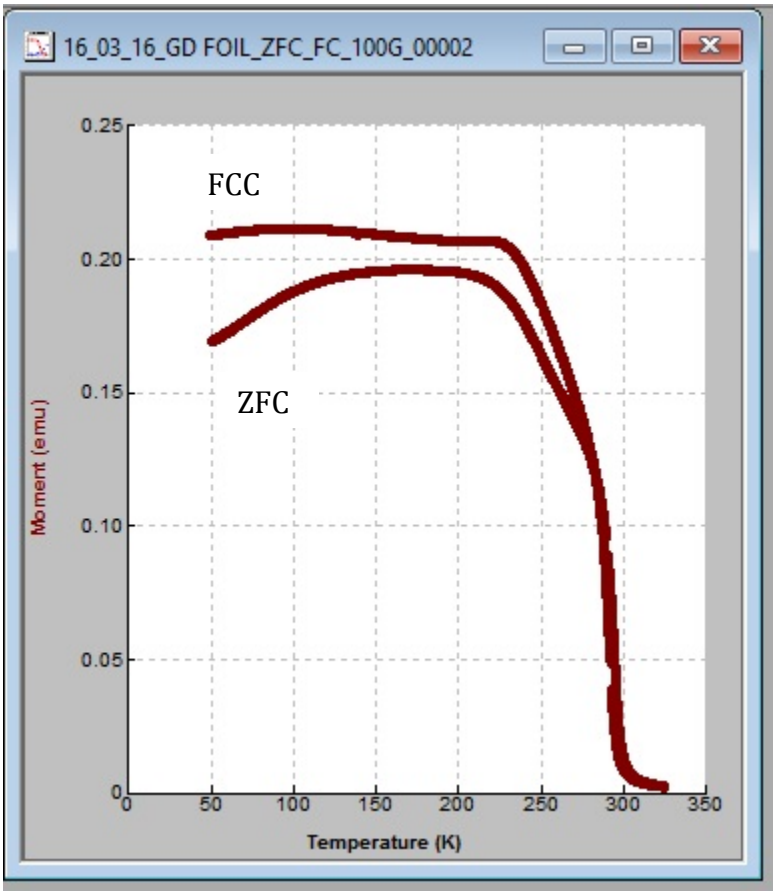


Figure 7. Moment vs. temperature data for the Gd foil with the ZFC being the down-turned plot and the FCC being the upper plot. Gaps in the high temperature data may be due to the re-centering of the sample holder during measurement.

**Antiferromagnetism:**

Antiferromagnets, like ferromagnets, exhibit long range magnetic order, but whereas ferromagnetic moments tend to align, neighboring antiferromagnetic moments tend to align oppositely, thereby canceling each other and producing very small magnetizations. Above the Néel temperature $T_N$, an antiferromagnet behaves like a paramagnet. Below $T_N$, the susceptibility is reduced with temperature [2].

Mn is an easily obtained materials with a Néel temperature of 100 K, as indicated in the Quantum Design periodic table of elements [Figure 1]. A sample of Mn was obtained, but with oxidation on its exterior. As previously explained, the magnetic moment v. H behavior is that of a paramagnet (Figure 8).

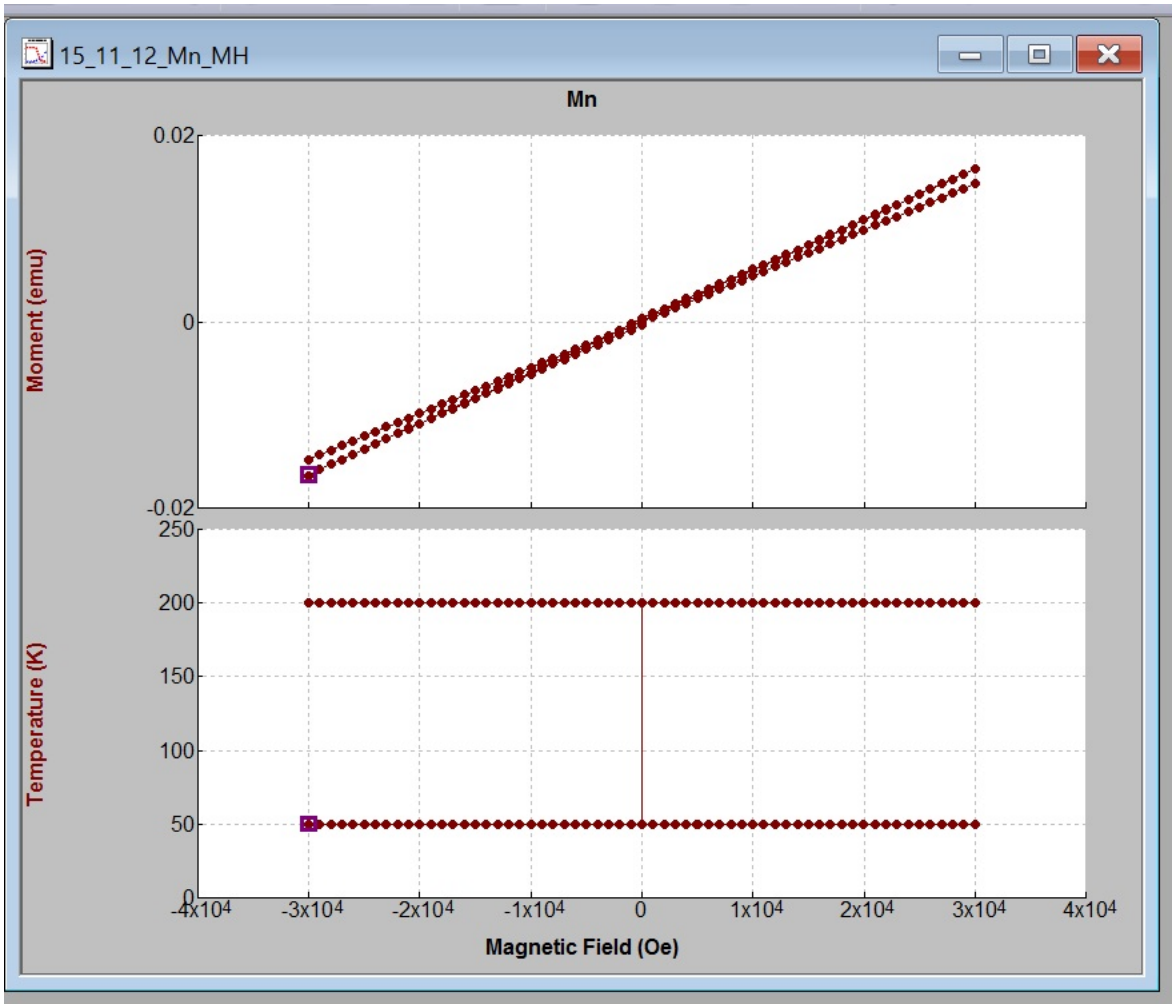


Figure 8. The square signifies the plot taken at 50 K, whereas the other plot is measured at 200 K. It can therefore be seen that the moment vs. field behavior both above and below $T_N$ is similar to that of a paramagnet. This plot demonstrates the versatility of MultiVu in plotting both data and instrument settings within the same display.

The magnetic moment vs. temperature plot is shown in Figure 9 below. The plot from just 90 K to 300 K is expected of a paramagnetic-antiferromagnet transition and indicates $T_N$ is approximately 130 K. This could be due to the presence of oxide, as MnO single crystal has been reported to have $T_N$ of 116 K [8]. The sharp "Curie tail" rise at low temperature is likely due to a paramagnetic impurity in the sample.

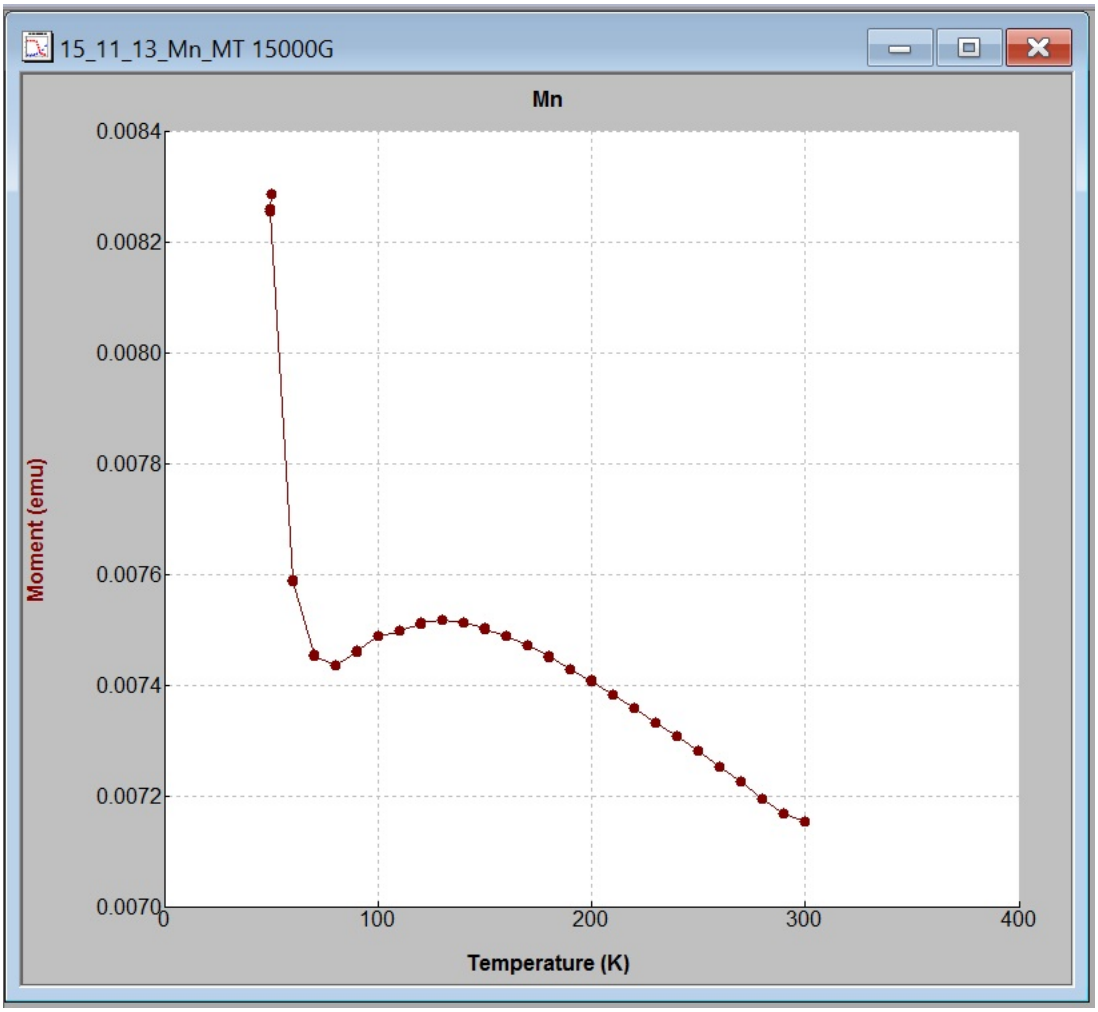


Figure 9. The magnetic moment vs. temperature for Mn with oxidation on its surface performed at 1.5 T. The low temperature region indicates the presence of an impurity.

**Diamagnetism:**

Whereas a paramagnet has a positive M(H) curve slope and is attracted to a magnetic field, a diamagnet has a negative M(H) curve slope and is repelled by a magnetic field. Diamagnetic materials have no net magnetic moment in the absence of an applied field and result from closed shell electron orbits. The theory set forth by Langevin in 1905 demonstrates that an applied magnetic field on a single electron orbit reduces the effective current of the orbit and therefore produces a magnetic moment that opposes the applied magnetic field [2]. The result is a material that exhibits "negative magnetism."

A sample of pyrolytic graphite was mounted using varnish on a brass holder with the c-axis perpendicular to the field. The moment vs. field (Figure 10, left) indeed has slope opposite to paramagnets. The sample was also mounted with the

magnetic field parallel to the c-axis, using a generous amount of GE varnish to hold the sample in the trough of the brass holder (Figure 10, right). Note that the moment with the field parallel to the c-axis is greater than that in the a-b plane, as is reported in the literature [9]. You may consider spending more to obtain a sample of highly oriented pyrolytic graphite (HOPG) for this measurement.

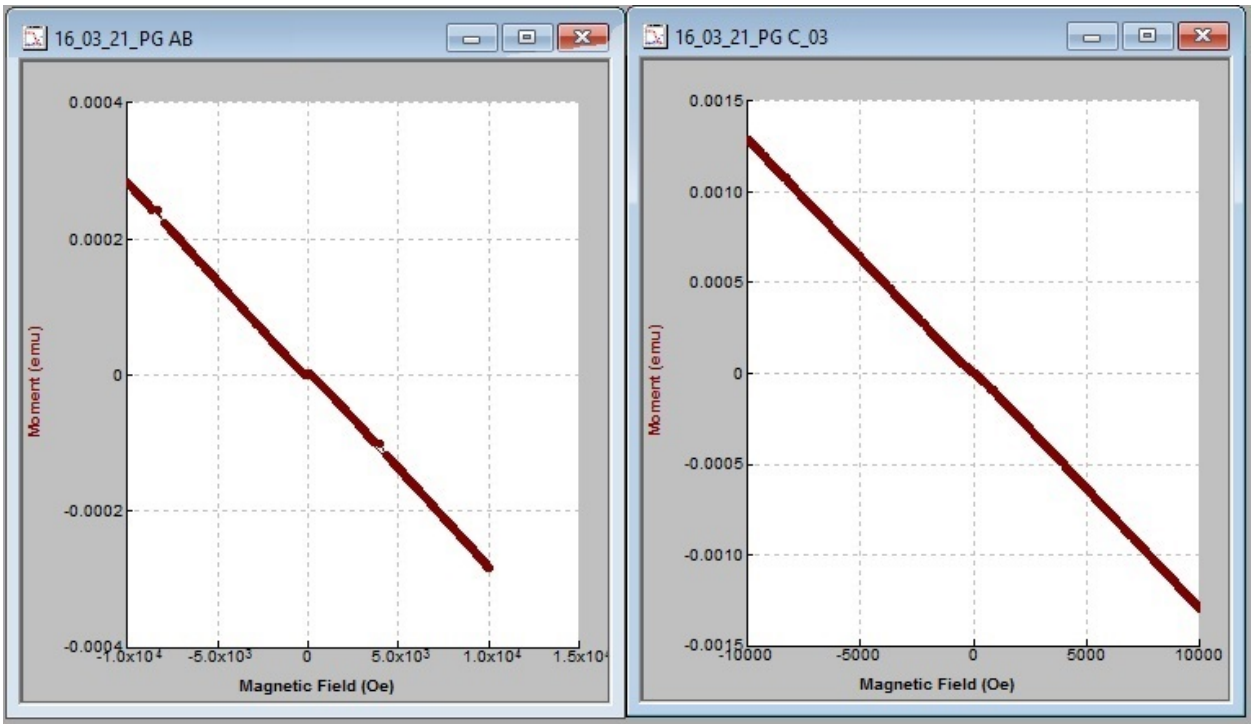


Figure 10. Moment vs. H for a sample of pyrolytic graphite, oriented with the field perpendicular to the c-axis (left) and parallel to the c-axis (right), performed at 300 K. Note the stronger magnetic moment in the c-axis.

## Superconductivity:

Although superconductors are so named for their zero electrical resistivity, the transition from the normal to the superconducting state below the critical temperature $T_C$ is accompanied by zero internal magnetic flux density due to the supercurrent, which is called the Meissner effect. The Meissner effect arises experimentally as a bulk negative magnetization, or diamagnetic behavior [4]. Because the measurement of zero resistivity requires the attachment of measurement leads and low level electrical meters, it can be more convenient and reliable to verify superconductivity via the Meissner effect, especially for very small samples.

The Meissner effect is easily demonstrated in the VersaLab using $YBa_2Cu_3O_{7-\delta}$ (YBCO), a widely available high temperature superconductor with a transition temperature $T_C$ ~ 93 K. In fact, the synthesis and electrical characterization of

YBCO is covered in the QD educational module “YBCO Synthesis and Characterization” [10].

Figure 11 shows a ZFC and FCC moment vs. temperature plot of a small sample of polycrystalline YBCO synthesized in-house. The applied field was 100 Oe. Note that the ZFC plot demonstrates strong magnetic field exclusion, whereas the FCC plot with its smaller low temperature moment indicates flux trapping.

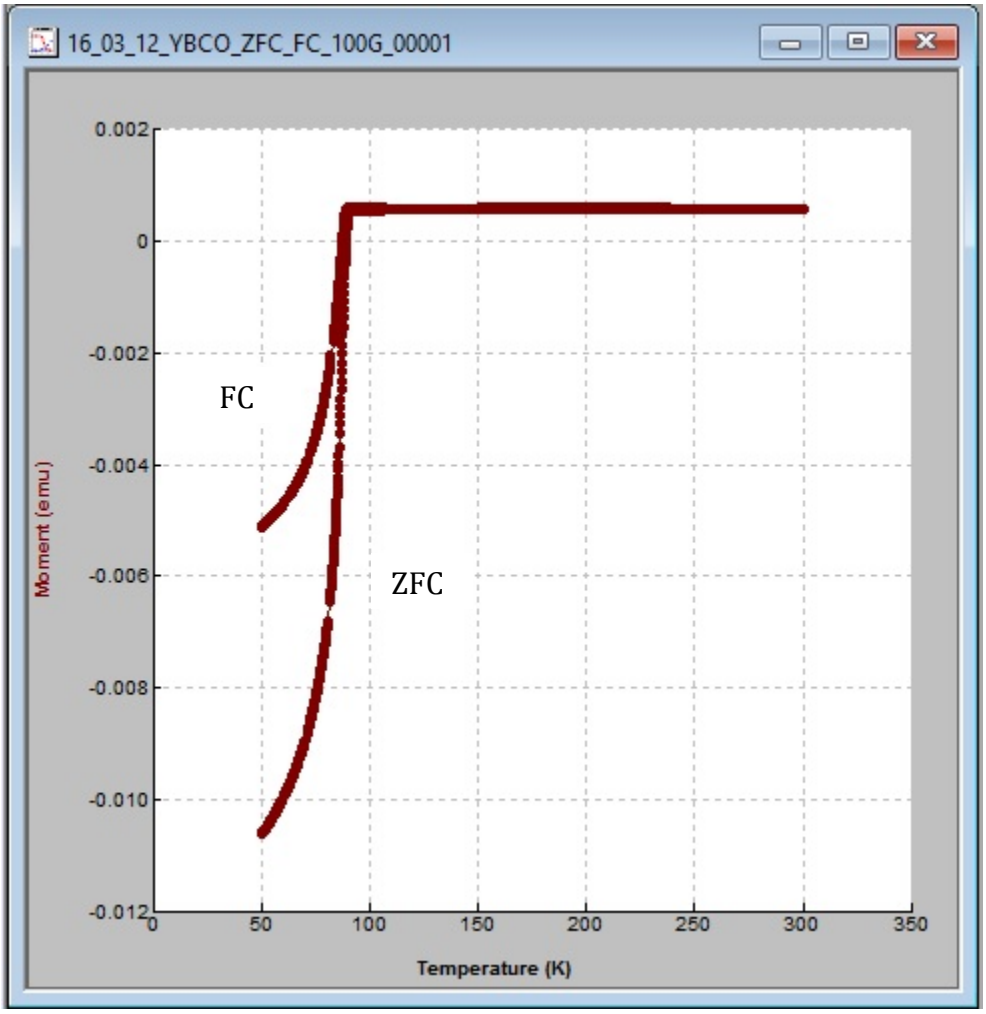


Figure 11. Moment vs. temperature data demonstrating the Meissner effect. The upper lower magnitude region is FCC, demonstrating flux trapping, while the more negative magnitude plot region is ZFC.

The critical temperature can clearly be seen at approximately 90 K. If your students have synthesized and measured YBCO using the ETO option, you may consider having them also run their samples on the VSM.

In the normal state, the M(H) behavior is paramagnetic (Figure 12).

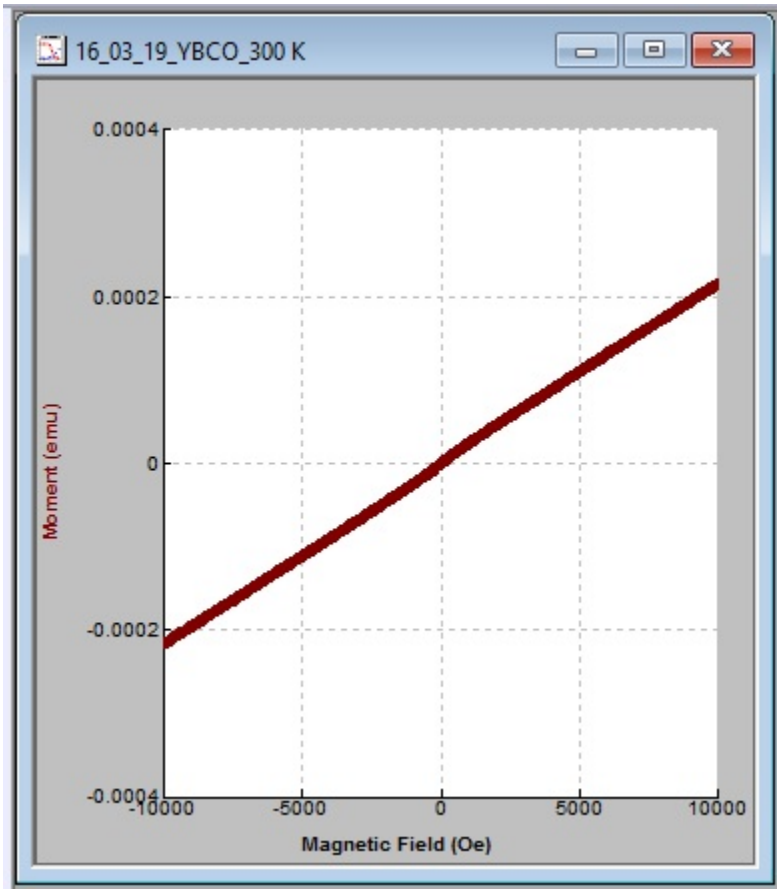


Figure 12. YBCO in the normal state possesses paramagnetic moment vs. field behavior.

Below $T_C$, the sample's superconductivity leads to more interesting behavior (Figure 13), with high field M(H) irreversibility due to "flux pinning". A reversible M(H) curve in this high field region indicates no flux pinning since magnetic flux passes in and out of the superconductor freely, while irreversibility results from the trapping of magnetic flux vortices at defects in the material. In fact, creating superconductors with high flux pinning is desirable for applications such as electrical power transmission and superconducting solenoid magnets. In addition, the familiar demonstration of the floating magnet above a superconducting YBCO puck relies on flux pinning to keep the magnet in place above the YBCO.

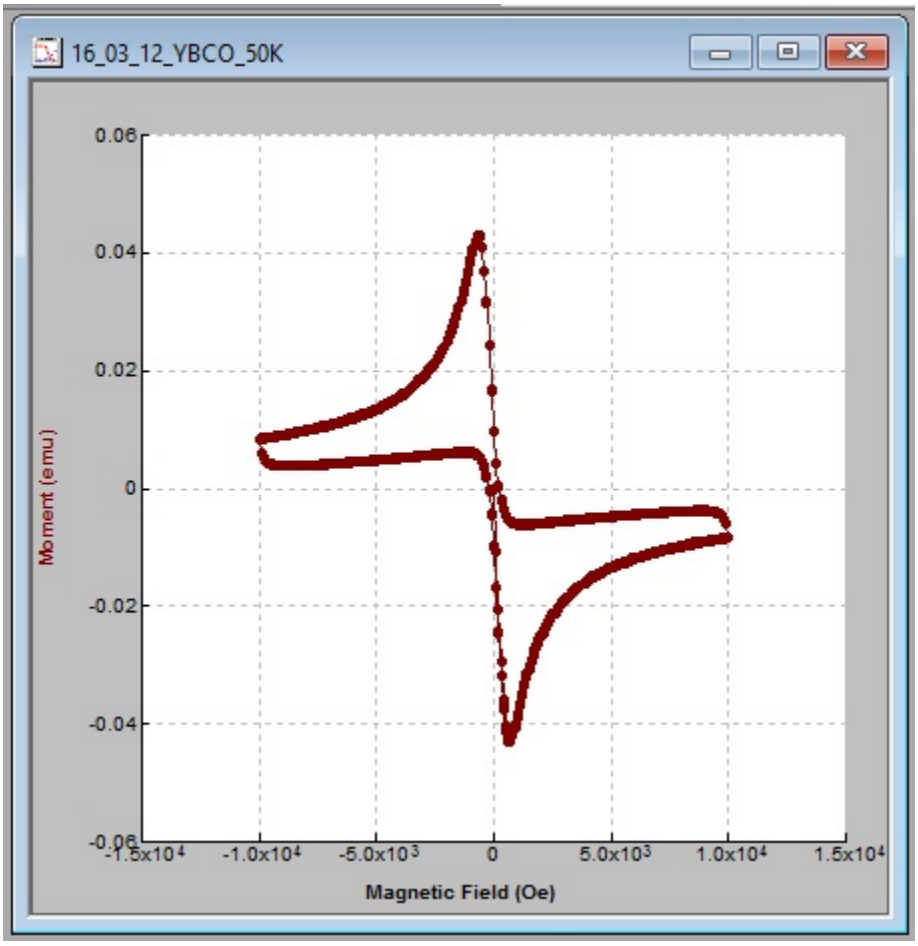


Figure 13. Moment vs. field data below $T_C$ at 50 K showing hysteresis in the mixed state in a Type II superconductor.

For a Type II superconductor, the supercurrent screens the sample by taking on a negative magnetic moment up to the lower critical field $H_{C1}$. As the applied field increases beyond this limit, the magnetic moment will decrease until it reaches the upper critical field $H_{C2}$, beyond which the superconductor enters the normal state [2]. To illustrate, we zoom in on the low field region of Figure 13 in Figure 14, to show $H_{C1}$ occurring at 600 Oe.

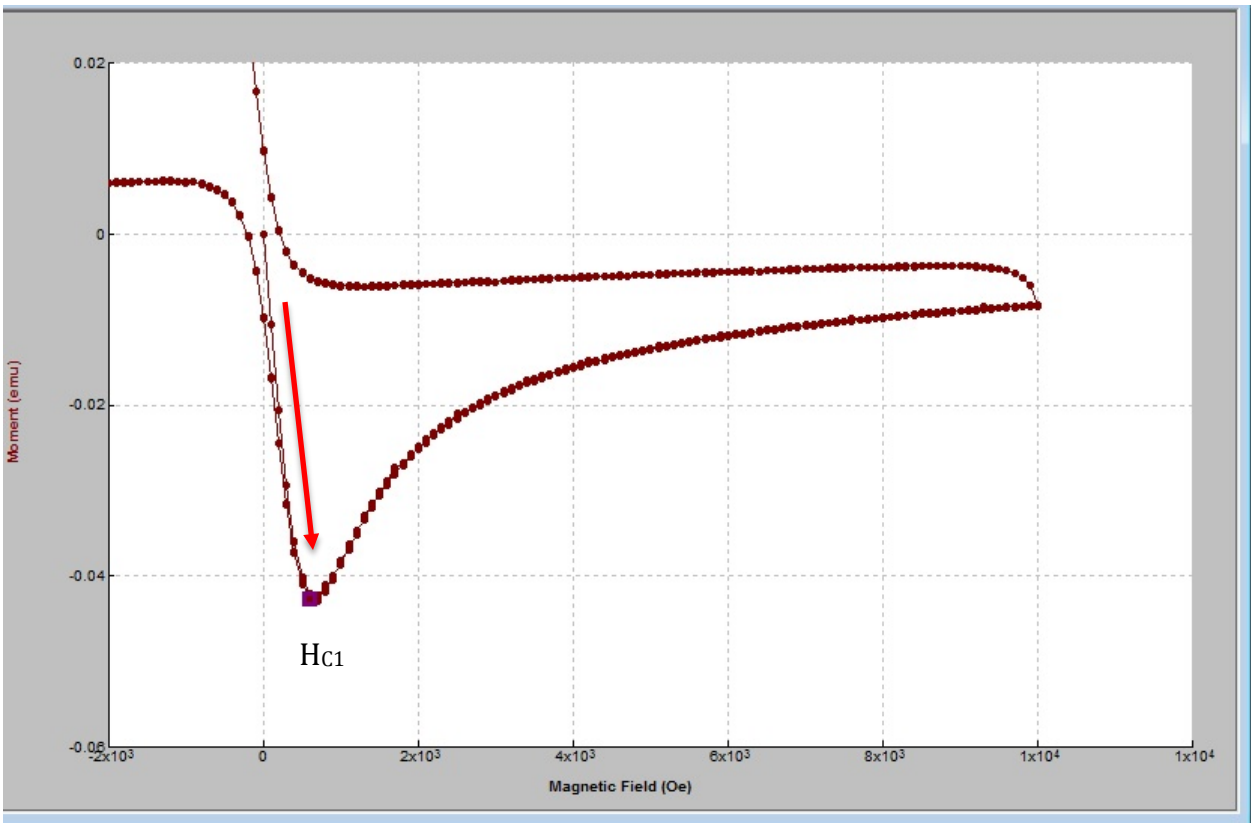


Figure 14. Plot showing the magnetic moment of superconducting YBCO measured at 50 K. Note the linear drop in moment until the field reaches $H_{C1}$ at approximately 600 Oe followed by the decreased magnitude in the mixed state.

**References:**

1. The Quantum Design Periodic Table of Elements located at http://www.qdusa.com/sitedocs/Quantum_Design_Periodic_Table.pdf
2. M. McElfresh, "Fundamentals of Magnetism and Magnetic Measurements" (1994). https://www.qdusa.com/sitedocs/appNotes/mpms/FundPrimer.pdf
3. "VSM Sample Mounting Techniques," QD Application Note 1096-306, http://www.qdusa.com/sitedocs/appNotes/ppms/1096-306.pdf
4. B.D. Cullity and C.D. Graham, *Introduction to Magnetic Materials*, 2nd Ed., IEEE Press (2009).
5. D.-X. Chen, V. Skumryev, and B. Bozzo, "Calibration of ac and dc magnetometers with a $Dy_2O_3$ standard," *Review of Scientific Instruments* 82, 045112 (2011).
6. S.Y. Dankov, A.M. Tishin, V.K. Pecharsky, and K.A. Gschneider, "Magnetic phase transitions and the magnetothermal properties of gadolinium," *Physical Review B* 57, 3478 (1998).
7. P.A. Joy, P.S. Anil Kumar, and S.K. Date, "The relationship between field-cooled and zero-field-cooled susceptibilities of some ordered magnetic systems," *Journal of Physics: Condensed Matter* 10, 11049 (1998).

8. T.R. McGuire and R.J. Happel, "The magnetic susceptibility of a MnO single crystal," *Journal de Physique et Le Radium* 20, 424 (1959).
9. J. Heremans, C.H. Olk, and D.T. Morelli, "Magnetic susceptibility of carbon structures," *Physical Review B* 49, 15122 (1994).
10. S. Tsui, "YBCO Synthesis and Characterization," QD Education Module, http://education.qdusa.com/experiment5.html

**Materials List:**

| Material | Amount Measured | Source | Catalog Number |
|---|---|---|---|
| $Dy_2O_3$ | | Alfa Aesar | 11319 |
| Ti foil | .005 g | Alfa Aesar | 13976 |
| Gd foil | .0092 g | Alfa Aesar | 12395 |
| Mn | .087 g | Alfa Aesar | 10236 |
| Pyrolytic Graphite | .0113 g | MTI Corporation | PG101005S1 |
| YBCO | .03 g | Synthesized in-house | |
| Kapton tape | | Quantum Design | |
| GE 7301 varnish | | Lakeshore | VGE-7031 |